Brain Pathology ISSN 1015-6305

RESEARCH ARTICLE

Cerebrovascular miRNAs correlate with the clearance of Aβ through perivascular route in younger 3xTg-AD mice

Lijuan Fu[1]; Ge Jiang[1]; Hope Weng[1]; Gregory M. Dick[1]; Yanzhong Chang[2]; Ghassan S. Kassab[1]

[1] California Medical Innovations Institute, San Diego, USA.
[2] Laboratory of Molecular Iron Metabolism, College of Life Science, Hebei Normal University, Shijiazhuang, China.

Keywords
3xTg-AD mice, Alzheimer's disease (AD), amyloid-β (Aβ), perivascular drainage, vascular miRNAs.

Abbreviations
ABCB1, ATP-binding cassette sub-family B member 1; Akt, also known as PKB, namely Protein kinase B; BSA, bovine serum albumin; Ct, cycle threshold; DTT, dithiothreitol; EGTA, ethylene glycol tetraacetic acid; GAPDH, glyceraldehyde 3-phosphate dehydrogenase; HBSS, Hanks' balanced salt solution; JNK, c-Jun N-terminal kinases; MAPK, mitogen-activated protein kinase; PBS, phosphate-buffered saline; PCR, polymerase chain reaction; PDGFRβ, platelet-derived growth factor receptor beta; PI3K, phosphoinositide 3-kinases; PIK3R2, phosphoinositol-3 kinase regulatory subunit 2; PMSF, phenylmethylsulfonyl fluoride; PTEN, phosphatase and tensin homolog; RNA, ribonucleic acid; s.c. injection, subcutaneous injection; SPRED1, sprouty related EVH1 domain containing 1; VEGFA, vascular endothelial growth factor A.

Corresponding authors:
Ghassan S Kassab, PhD, President and Professor of California Medical Innovations Institute, 11107 Roselle Street, San Diego, CA 92121 (Email: *gkassab@calmi2.org*)
Lijuan Fu, PhD, California Medical Innovations Institute, 11107 Roselle Street, San Diego, CA 92121 (Email: *lfu@calmi2.org*)

Received 19 February 2019
Accepted 4 June 2019
Published Online Article Accepted 17 June 2019

doi:10.1111/bpa.12759

Abstract

The "two-hit vascular hypothesis for Alzheimer's disease (AD)" and amyloid-β (Aβ) oligomer hypothesis suggest that impaired soluble Aβ oligomers clearance through the cerebral vasculature may be an initial step of the AD process. Soluble Aβ oligomers are driven into perivascular spaces from the brain parenchyma and toward peripheral blood flow. The underlying vascular-based mechanism, however, has not been defined. Given that microRNAs (miRNAs), emerging as novel modulators, are involved in numerous physiological and pathological processes, we hypothesized that cerebrovascular miRNAs may regulate the activities of brain blood vessels, which further affects the concentration of Aβ in the AD brain. In this study, perivascular Aβ deposits, higher vascular activation, increased pericyte coverage and up-regulated capillaries miRNAs at 6 months old (6 mo) were found to correlate with the lower Aβ levels of middle AD stage (9 mo) in 3xTg-AD (3xTg) mice. It is implicated that at the early stage of AD when intracellular Aβ appeared, higher expression of vessel-specific miRNAs, elevated pericyte coverage, and activated endothelium facilitate Aβ oligomer clearance through the perivascular route, resulting in a transient reduction of Aβ oligomers at 9 mo. Additionally, ghrelin-induced upregulation of capillary miRNAs and increased pericyte coverage attenuated Aβ burden at 9 mo, in further support of the relationship between vascular miRNAs and Aβ clearance. This work suggests a cerebral microvessel miRNA may boost endothelial highly activated phenotypes to promote elimination of Aβ oligomers through the perivascular drainage pathway and contribute to AD progression. The targeting of brain vessel-specific miRNAs may provide a new rationale for the development of innovative therapeutic strategies for AD treatment.

INTRODUCTION

Alzheimer's disease (AD), as one of the most important neurodegenerative disorders, is a world-wide problem that currently has no cure. It is reported that over 40% of US individuals above 85 years old have been diagnosed with AD (55). The causes of most AD cases are still not fully understood except for the ~5% of early-onset familial AD (FAD) cases that have been identified by aberrant alleles (10). There are several competing hypotheses to explain the cause of AD. The general consensus, namely "Amyloid (Aβ) Cascade Hypothesis" (19), suggests that imbalances in Aβ metabolism promote the aggregation of Aβ in the brain, initiating neurodegeneration and cognitive impairment in AD. Proponents advocate the overproduction and processing of Aβ precursor protein (APP) and impaired elimination of Aβ from the brain lead to the accumulation of Aβ peptide which condenses and becomes insoluble fiber (fibril) to form senile plaque, resulting neuronal damage and the symptoms of AD. A series of clinical trials based on amyloid reduction therapy failed to deliver the anticipated clinical improvement in mild-to-moderate AD, raising legitimate concerns for the validity of this hypothesis.

The recent "oligomer hypothesis" suggests that the condensation process of soluble Aβ oligomer causes steady memory loss mediated by synaptic injury. (2, 34). Several different forms of Aβ, such as monomers, oligomers and fibrils, exist in AD brains and are constantly dynamic. Several possible clearance systems that act together to drive extracellular soluble Aβ oligomers from the brain have been described in the previous studies. These include enzymatic degradation, cellular uptake, blood–brain barrier (BBB) transportation, interstitial fluid (ISF, that surrounds neurons) bulk flow and cerebrospinal fluid (CSF, that surrounds the brain) absorption by the circulatory and lymphatic drainage (37, 55). The perivascular route exists in the spaces around the brain vasculature and is a path for delivering all the essential substances the cells require and allows the efflux of unwanted wastes, such as Aβ, through the ISF bulk flow. Soluble Aβ oligomers in the ISF flow are driven by arterial pulsation into the perivascular space located along the smooth muscle cells (SMCs) and capillary basement membrane and toward the subarachnoid space, and ultimately out of the brain (3, 14, 30, 37).

Several challenges, particularly significant gaps of knowledge in the biological mechanisms of AD, however, impede the discovery of effective drugs for AD treatment. Neurovascular network damage in AD has been suspected for a long time. A large body of data indicates that brain blood vessel dysfunction is a vital pathological trait of AD among the earliest clinical biomarkers (4, 15, 23–25, 48, 58, 65, 72). The "Two-hit vascular hypothesis for AD" suggests signs of cerebrovascular pathology may be the initial steps of AD process. Dysfunctional cerebral vasculature may promote faulty Aβ clearance and precede the appearance of Aβ-initiated neuronal injury and cognitive impairment (53). The multifaceted pathogenesis of AD implicates a complex interaction among numerous microenvironment insult stimuli and responsive cell types. The complexity of the cerebrovascular network requires coordinated genetic programs that are partly controlled by transcriptional activity. The endogenous non-coding RNAs, such as microRNAs (miRNAs, ~22 nt) modulate gene expression at the post-transcriptional level in series of the biological program and modify multiple-actions through regulating multiple-molecular cascades (13, 28, 32, 61) in many complex multi-factors diseases have been utilized to impact both cardiovascular diseases and AD (13, 26, 38, 46, 47, 57).

How cerebrovascular miRNAs regulate the expression of intracellular genes of the vessel wall, which in turn affect Aβ oligomer aggregation in AD brains remains unknown. To address this question, we have screened 11 capillary miRNAs closely related with both cardiovascular diseases and AD. The five most abundant and significantly changed miRNAs were selected to analyze the relationship between the functional activation of the cerebral vasculature and their expression patterns in different AD phases of 3xTg mice. Ghrelin, known as the "hunger hormone," is a neuropeptide generated from ghrelinergic cells of the gastrointestinal tract. It has numerous functions, including appetite stimulation, increase in food intake and fat storage, as well as regulation of energy homeostasis (1, 8). Furthermore, since ghrelin is thought to stimulate angiogenesis in ischemic muscles by inducing miRNAs upregulation (29), ghrelin was administered via subcutaneous injection (s.c. injection) to induce upregulation of miRNAs at the stage of lower vascular activities in AD brains to verify the relationship between selective vascular miRNAs and Aβ clearance. The findings of this work provide a more integrative understanding of the cellular and molecular progression in the pathology of AD which may enhance the development of cerebrovascular miRNA-targeting strategies aimed at ameliorating the dysfunction of brain–blood vessels in AD brain.

MATERIALS AND METHODS

Animals

Triple transgenic mice, 3×Tg–AD, containing three mutations (PEN1 M146, APP Swedish and MAPT P301L), are widely used as an animal model of FAD. Age and gender-matched B6129SF2/J strain were used as the wild type (WT) control. Mice were obtained from the Jackson Laboratory and bred in our research institute's animal facility. Mice were housed in plastic cages on a 12/12 h light/dark cycle with ad libitum access to water and standard rodent diet. Animal usage was approved by California Medical Innovations Institute (CalMI2) Institutional Animal Care and Use Committee (IACUC). The genotyping was conducted in CalMI2 animal facilities at the age of 21 days by tail DNA extraction according to our previous protocol (67, 70) and the online information supplied by the vendor. Eleven mice per strain

(3xTg-AD, B6129SF2/J) at the ages of 6, 9 and 12 mo were used in this study. In the ghrelin administration study, 3xTg-AD mice aged 9 mo received s.c. injections of either n-octanoylated ghrelin (AnaSpec, 600 μg/kg per day, n = 6–8) or saline every 2 days for 2 weeks.

Capillaries isolation

Capillaries were isolated as previously described (5). Mouse brains were carefully isolated and the meninges were removed in ice-cold Hanks' balanced salt solution (HBSS) containing 1% bovine serum albumin (BSA). The cortex and hippocampus were macroscopically dissected and all visible white matter was discarded. Tissues were then minced and homogenized in HBSS containing 1% BSA with a glass-douce homogenizer on ice. Dextran (70 kDa, Sigma) was subsequently added to yield a final concentration of 16% and the samples were thoroughly mixed, followed by centrifugation at 6000 g for 15 minutes. The microvessel-depleted brain remaining on top of the Dextran gradient was collected for Aβ identification, and the capillary pellets located at the bottom of the tubes were harvested. Due to the small yields of capillaries per mouse, the capillary pellets from two animals were pooled and sequentially filtered through a 100 and 6 μm cell strainer (pluriSelect). The capillaries remaining on top of the 6 μm cell strainer were collected in HBSS buffer and either lysed to collect total RNA for real-time polymerase chain reaction (PCR) or smeared on glass slides for fluorescent staining analysis.

Microvessels immunofluorescent detection

The isolated microvessel fragments were smeared onto Superfrost Plus pre-cleaned glass microscope slides and fixed using ICC Fixation Buffer (BD Pharmingen) for 15 minutes at room temperature (RT). The microvessels were then rinsed with phosphate-buffered saline (PBS) and blocked in PBS containing 0.3% Triton X-100 and 5% donkey serum (Jackson ImmunoResearch) for 1 h at RT followed by incubation with the primary antibodies [mouse anti-platelet-derived growth factor receptor beta (PDGFRβ) for staining pericytes, R&D systems; mouse anti-LRP1 (low-density lipoprotein receptor-related protein 1), RAGE (receptor for advanced glycosylation end products) and Mdr1 (multidrug resistance protein 1, also known as ATP-binding cassette sub-family B member 1 [ABCB1]) for detecting the transporters of Aβ on the BBB, Santa Cruz] overnight at 4°C. The slides were washed and incubated with the secondary antibodies (Alexa Fluor 546 conjugated donkey anti-mouse secondary antibody, Invitrogen) diluted in 1% donkey serum containing DyLight 488 Labeled Lycopersicon Esculentum Lectin (1:200, Vector Laboratories) for 1 h at RT. For coverage analysis, the percentage of PDGFRβ-positive pericyte area covering lectin-positive capillary area was quantified using Image J Area analysis as described previously (5). For the expression analysis of Aβ transporters, the area of LRP1, RAGE and Mdr1-occupied endothelium were measured as an area percentage normalized by the total area of lectin-positive capillaries using Image J Area measurement tool (5). A total of 15–30 images were collected from each slide, and 6 mice per group were used for statistical analysis. Analysis of images was conducted blindly.

Tissue immunofluorescent staining

Mice were anesthetized with 1–2% isoflurane by inhalation. Intracardiac perfusion with 100 mM PBS (pH = 7.4) containing 5 U/ml heparin was performed and followed by 4% fresh paraformaldehyde (PFA) in 100 mM PBS. The brains were dissected and maintained in 4% PFA at 4°C until sectioning. Perfused brains were embedded into Richard-Allan Neg 50 Frozen Section Medium (Thermo Scientific) in liquid nitrogen. Embedded frozen brain tissue was cryo-sectioned at a thickness of 14 μm. For staining Aβ with 6E10 and 4G8 antibodies, sections were pretreated with formic acid solution (70%) at RT for 15 minutes to perform antigen retrieval. Then, sections were blocked with 5% donkey serum for 60 minutes and incubated with primary antibodies (6E10 and 4G8 for recognizing all forms of amyloid, Biolenged; A11 for detecting soluble Aβ oligomers, Rockland; anti-Aβ fibril, Abcam; anti-CD68 and CD3ε for mainly labeling the macrophages and T cells, respectively, Santa Cruz) diluted in 1% donkey serum overnight at 4°C. Given the A11 antibody was produced from whole rabbit serum prepared by repeated immunizations with a synthetic molecular mimic of soluble oligomers according to manufacturer's instructions, it can specifically recognize all types of amyloid oligomers, but not detect native proteins, amyloidogenic monomers or mature amyloid fibrils. Washed slides were incubated in secondary antibodies (Alexa Fluor 546 conjugated donkey anti-rabbit and anti-mouse secondary antibody, Alexa Fluor 488 conjugated donkey anti-mouse secondary antibody, Invitrogen) with DyLight 488 Labeled Lycopersicon Esculentum Lectin (1:200, Vector Laboratories) and Hoechst 33342 stain (1:5000, Invitrogen) 1 h. at RT. Slides were washed, and coverslips were mounted by Shandon Immu-Mount (Thermo Scientific). Fluorescence was visualized and photographed by Nikon ECLIPSE TE300 with ISCapture software and Nikon ECLIPSE Ts2R with NIS Elements software. To analyze Aβ aggregated-vessels and vascular activation, the number of $A11^+$, $CD3\varepsilon^+$ and $CD68^+$ vessels of Lectin-positive endothelium were counted and expressed as the average number of $A11^+$, $CD3\varepsilon^+$ and $CD68^+$ vessels in Lectin-labeled endothelium. The capillary density was analyzed by counting the number of capillary branches. Five animals per group and 6–8 randomly selected fields from the cortex and hippocampus in 6 nonadjacent sections of each animal were used for statistical analysis.

Reverse transcription and quantitative real-time PCR analysis

Total RNA was purified with Trizol reagent (Invitrogen), according to the manufacturer's instructions. To quantify miR-126-3p (MIMAT0000138), miR-145-5p (MIMAT0000157),

miR-195-5p (MIMAT0000225), miR-21-5p (MIMAT0000530) and miR-29b-3p (MIMAT0000127), reverse transcription and quantitative PCR (qPCR) were performed using the TaqMan@ microRNA assay kit (Applied Biosystems) as previously described (20, 51). Briefly, reverse transcription was performed in a 15 μl reaction mix containing 10 ng of total RNA, 3 μl of miRNA primer mix, 1 mM dNTP, 50 U reverse transcriptase, and 3.8 u. RNase inhibitor. Reactions were incubated at 16°C for 30 minutes, and 42°C for 30 minutes followed by 85°C for 5 minutes. The PCR was performed in a 10 μl reaction volume containing 0.5 μl of miRNA primer and TaqMan probe mix, 0.67 μl of RT product (diluted fivefold) and 5 μl of TaqMan Universal PCR Master Mix. The cycling conditions were as follows: 10 minutes at 95°C followed by 40 cycles of 15 s at 95°C and 1 minute at 60°C. U6 small RNA was used as an internal control following the manufacturer's recommendation. For all samples, reverse transcription and qPCR were performed three times and qPCR was performed in triplicate. Relative gene expression levels between WT and 3xTg-AD mice were determined using the comparative cycle threshold ($2^{-\Delta\Delta Ct}$) method after normalizing to U6.

Immunoblotting analysis

The method has been described previously (22, 60). Briefly, microvessel-depleted cortex and hippocampus tissues (75 μg per lane) were homogenized in lysis and extraction buffer containing 50 mM β-glycerophosphate, 0.1 mM Na_3VO_4, 2 mM $MgCl_2$, 1 mM ethylene glycol tetraacetic acid, 1 mM dithiothreitol, 0.02 mM pepstatin, 0.02 mM leupeptin, and 1 mM phenylmethylsulfonyl fluoride, as well as 0.5% Triton X-100 and 0.1 U/ml aprotinin. After centrifugation at 12 000 rpm for 20 minutes, protein content was determined by Bradford assay. Protein samples were separated by 4–12% Bis-Tris gels (Life Technologies) and then transferred to nitrocellulose membranes (Bio-Rad), which were blocked 1 h. at RT with 5% bovine serum albumin Tris-buffered saline-Tween (0.5 M NaCl, 20 mM Tris–HCl, 0.1% (v/v) Tween 20, pH 7.6). Membranes were incubated overnight at 4°C in buffer containing primary antibody (1:1000 for A11, Rockland, and 1:2000 for glyceraldehyde 3-phosphate dehydrogenase (GAPDH), Santa Cruz) followed by horseradish peroxidase-conjugated secondary antibody. The A11 antibody was used to detect the high molecular weight Aβ oligomer specifically. GAPDH (a loading control) and A11 immunoreactivity were visualized with ECL Prime (Amersham) according to the manufacturer's instructions. The experiments were repeated at least three times.

Aβ oligomer enzyme-linked immunosorbent assay

Human Aβ oligomers were analyzed in the microvessel-depleted cortex and hippocampal supernatant by enzyme-linked immunosorbent assay (ELISA; IBL International, Germany) according to manufacturer's instructions. The ELISA uses mouse monoclonal anti-human Aβ (N) (82E1) antibodies that recognize the N-terminus of human Aβ specifically, with 2 or more epitopes.

Statistical analysis

All images were prepared using Adobe Photoshop CS5. Statistical analysis was performed using SPSS 21.0. Results were expressed as mean ± SEM. The difference between two data sets was determined using Student's t-test, with $P < 0.05$ indicating statistical significance.

RESULTS

Aβ oligomer-laden cerebral blood vessels were present in young 3xTg mice

The number of vessels per 5 mm^2 in the cerebral cortex and hippocampus were evaluated as the density of capillaries (diameter ≤10 μm, labeled by Lectin), which were significantly reduced ($P < 0.001$) in AD mice brains aged at either 6 mo or 12 mo compared to that of WT mice at the same ages (Figure 1E,H and quantified as shown in 1K). Interestingly, the number of blood vessels stained with A11 antibody in younger AD mice (6 mo) was much higher ($P < 0.05$) than that of WT mice at the same age (Figure 1L). The significant increase in Aβ oligomers was exclusively observed in the perivascular space of both larger vessels (diameter >50 μm) and capillaries (Figure 1F) at the early stage of AD mice (6 mo, Figure 1E,F), rather than the middle (9 mo, Figure 1G) or late (12 mo, Figure 1H) phases. The perivascular Aβ oligomer burden is reminiscent of cerebral amyloid angiopathy (CAA). Meanwhile, Aβ plaques appeared in both brain parenchyma (Figure 1I) and blood vessel walls (CAA in 20 mo, Figure 1J) at the advanced stage of AD.

Activated endothelium with positive immune cells around cerebral blood vessels in younger 3xTg mice

To determine the relationship of the removal of Aβ oligomers through the perivascular route and the neurovascular malfunction in AD brains, activated endothelium including activities of immune cells was detected by immunofluorescence staining. At 6 mo, robust CD3ε- and CD68-positive vessels were visualized ($P < 0.001$) at Lectin-labeled arterioles/venules in the cortex and hippocampus of AD brains (Figures 2B and 3B) in comparison with the WT brains (Figures 2A and 3A). CD3ε and CD68 are usually identified as markers for immunophenotyping of cells and appeared on T cells, macrophages, monocytes, neutrophils, basophils and large lymphocytes. Particularly at 9 mo, higher CD3ε-positive vessels were still aligned with microvessels ($P < 0.001$) in the AD brain (Figure 2D), while CD68-stained vessels disappeared in 3xTg samples (Figure 3D). CD3ε- and CD68-stained vessels were visible at the age of

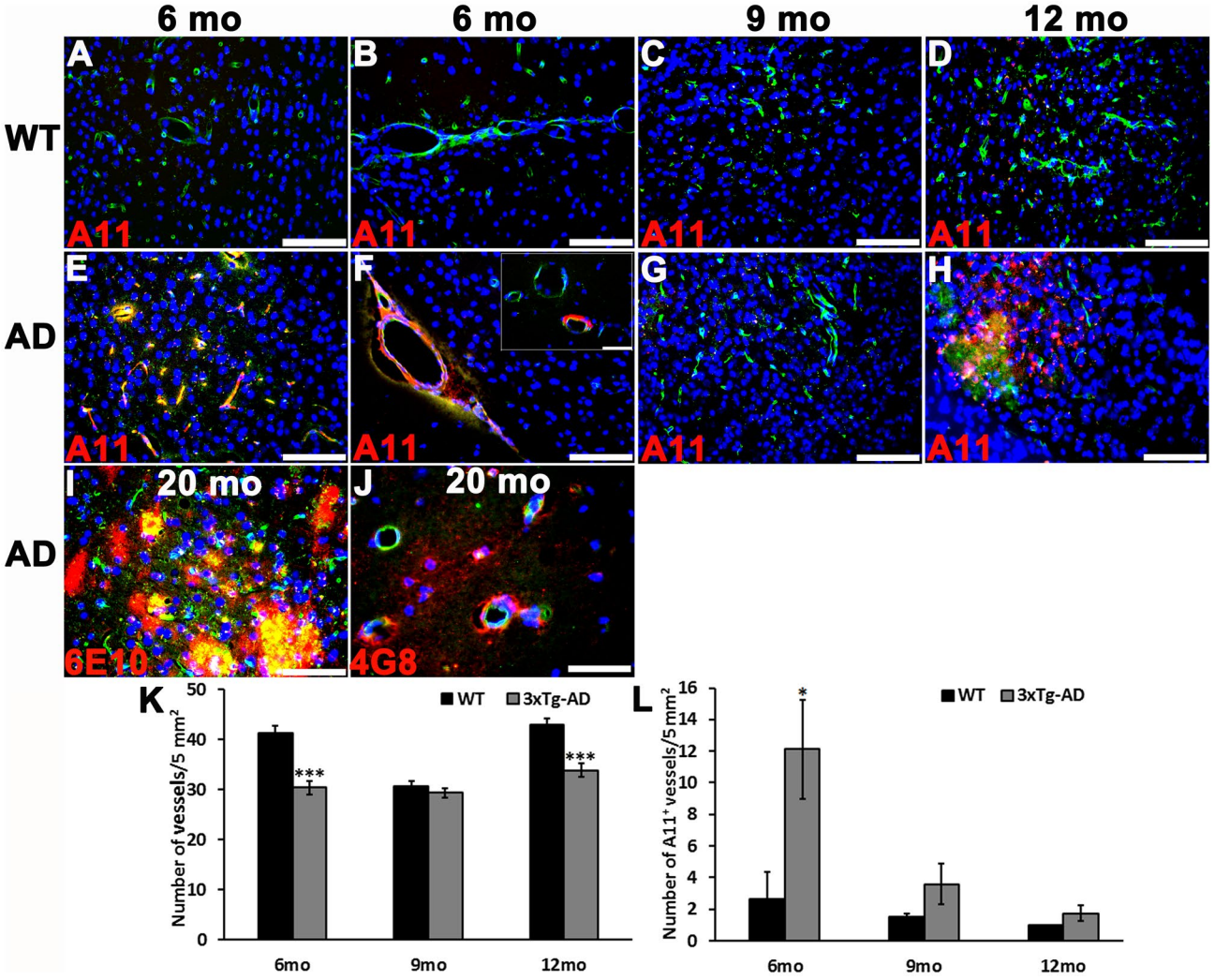

Figure 1. *The exclusive perivascular accumulation of Aβ in 3xTg mice brains aged 6 mo.* (**A-H**) A11 positive (Red) blood vessels labeled with Lectin (Green) in the cerebral cortex and hippocampus of WT (**A-D**) and 3xTg (**E-H**) mice aged 6 mo (**A, B** and **E, F**), 9 mo (**C** and **G**) and 12 mo (**D** and **H**). (**I-J**) Aβ plague stained with 6E10 (**I**) antibody (Red) and cerebrovascular aggregated Aβ (CAA) marked with 4G8 (**J**) antibody (Red) in 20 mo of AD mice brain. A11 antibody was used to stain the high molecular weight Aβ oligomers. Blue, Hoechst 33342 stained nuclear. Scale bar, 20 μm. (**K**) Capillary density of WT and AD (3xTg-AD) mice. (L) Quantitative analysis for the number of A11⁺ vessels in WT and AD brains. Error bars = SEM; $*P < 0.05$, $***P < 0.001$, Student's *t* test. n = 5 animals/group.

12 mo in WT brains (Figures 2E and 3E) although they were absent in AD brains ($P < 0.001$, Figures 2F and 3F). A high concentration of immune cells found in proximity to the cerebral vasculature (as shown in Figures 2B and 3B) suggests that endothelial activation and inflammation may be implicated in the progression of Aβ clearance and aggregation in the early AD mice.

Different expression patterns of Aβ at different AD stages in 3×Tg mice

From 6 through 12 months, our data showed a progressive increase in intracellular Aβ accumulation of the cerebral cortex and hippocampus region (Figures 4A-C) stained with 6E10 antibody. Interestingly, we found the levels of toxic Aβ oligomers transiently decreased at 9 mo using A11 antibody (Figure 4H) and anti-Aβ fibril antibody (that can identify all forms of Aβ, Figure 4E) for immunofluorescent staining. To determine whether the transient decrease in Aβ oligomers at 9 mo is associated with perivascular elimination of Aβ oligomers and the temporal profile of vascular activation, we evaluated the morphological and molecular dysfunction of cerebral vasculature in this AD mice by measuring pericyte coverage and vessel-specific miRNAs levels.

Pericyte coverage in 3×Tg mice

We measured the pericyte coverage in capillaries (purification >90%, Figure 5A) isolated from the cerebral cortex

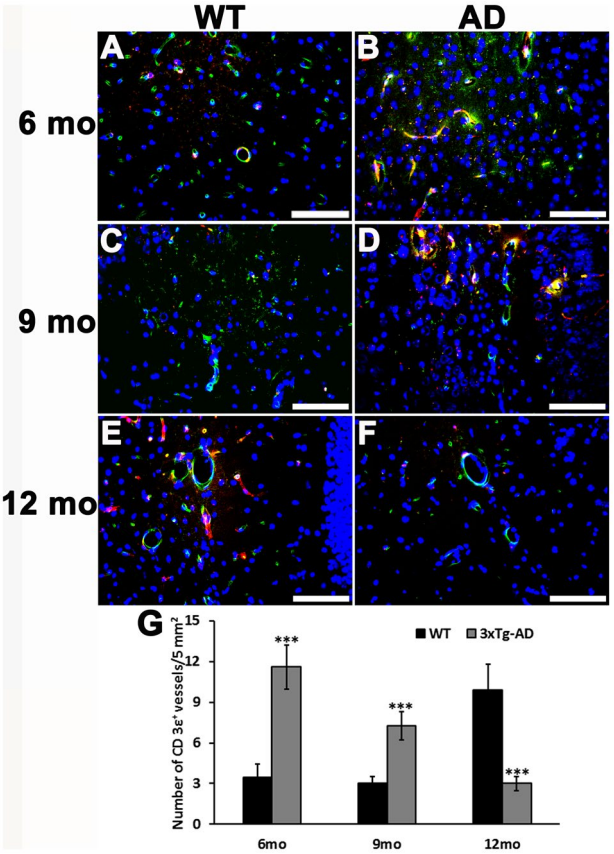

Figure 2. *Increased CD3ε⁺ vessels adjacent to cerebral vasculature in young AD mice brains.* (**A-F**) The representative images of CD3ε (Red) expressing blood vessels in the cerebral cortex and hippocampus of WT (**A, C** and **E**) and 3xTg (**B, D** and **F**) mice aged 6 mo (**A** and **B**), 9 mo (**C** and **D**) and 12 mo (**E** and **F**). Green, Lectin labeled blood vessels; Blue, Hoechst 33342 stained nuclear. Scale bar, 20 μm. (**G**) The quantitative comparison of the number of CD3ε⁺ vessels between 3xTg and WT mice. Error bars = SEM; ***$P < 0.001$, Student's *t* test. n = 5 animals/group.

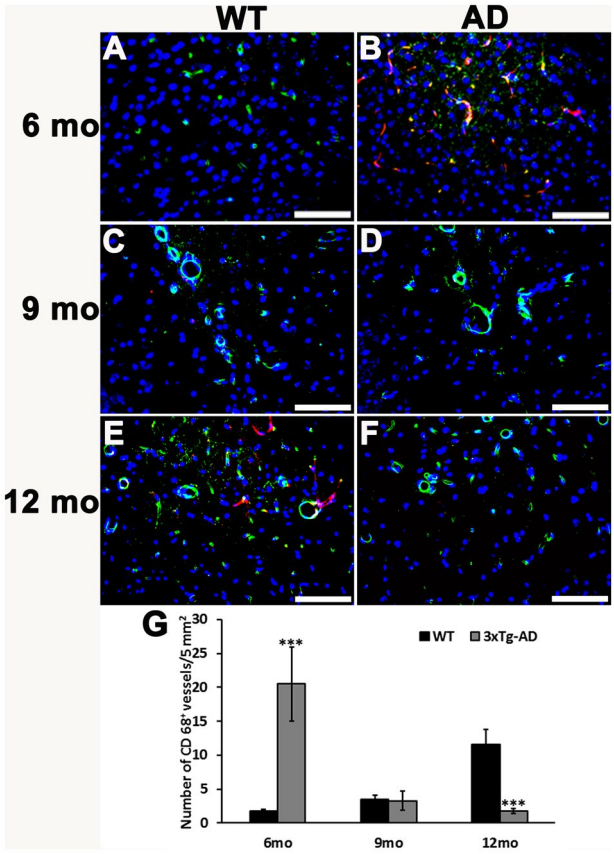

Figure 3. *Increment of CD68⁺ blood vessels observed in young AD mice brains.* (**A-F**) CD68⁺ (Red) blood vessels in the cerebral cortex and hippocampus of WT (**A, C** and **E**) and 3xTg (**B, D** and **F**) mice aged 6 mo (**A** and **B**), 9 mo (**C** and **D**) and 12 mo (**E** and **F**). Green, Lectin labeled blood vessels; Blue, Hoechst 33342 stained nuclear. Scale bar, 20 μm. (**G**) Measurement for the number of CD68⁺ vessels in 3xTg and WT mice brain. Error bars = SEM; ***$P < 0.001$, Student's *t* test. n = 5 animals/group.

and hippocampus of 6–12 mo 3×Tg and age-matched WT mice brain, verified by anti-PDGFR-β antibody and lectin (as shown in Figure 5B). The percentage of pericyte coverage was quantified as in Figure 5C. Coincidentally, the pericyte coverage significantly increased at the age of 6 mo ($P < 0.05$), decreased at 9 mo ($P < 0.001$) and increased again at 12 months ($P < 0.01$) in 3×Tg mice as compared to that of WT mice. Notably, an apparent increase in the pericyte coverage was observed in WT brains aged 9 mo. In addition, our findings indicate the elevation of pericyte coverage in 6 mo AD brain coincident with the appearance of Aβ-loaded blood vessels and vascular activation, closely correlating with the temporal profile of Aβ, especially the decrease in Aβ oligomers of 9 mo AD brains. In other words, pericyte coverage increased when intracellular Aβ appeared at 6 mo as well as the activated endothelium facilitate to drive Aβ oligomer clearance from the perivascular space, resulting in the transient reduction of Aβ oligomers at 9 mo.

Levels of miRNAs in isolated capillaries correlate with the clearance of Aβ via the perivascular route in 3×Tg mice

Capillaries from cerebral cortex and hippocampus were isolated using density-gradient centrifugation. A total of 11 miRNAs implicated in cardiovascular diseases and AD were screened (Figure S1A). Based on miRNAs qPCR assay (Figure S1B), levels of the 5 most abundant miRNAs in isolated microvessels, namely miR-126-3p, miR-145-5p, miR-195-5p, miR-21-5p and miR-29b-3p, were analyzed. These miRNAs increased (particularly miR-126 and 145, $P < 0.05$) at the age of 6 mo in AD brains (Figure 6A). All 5 miRNAs (miR-21, 145 and 195, $P < 0.05$; miR-29b and 126, $P < 0.01$) significantly decreased with the reduction of Aβ oligomers (9 mo, Figure 6B), followed by a slight increase (not significantly) when Aβ fibrils appeared (12 mo, Figure 6C). As seen in Figure 6D, miR-126 and miR-145 showed much lower threshold cycle numbers

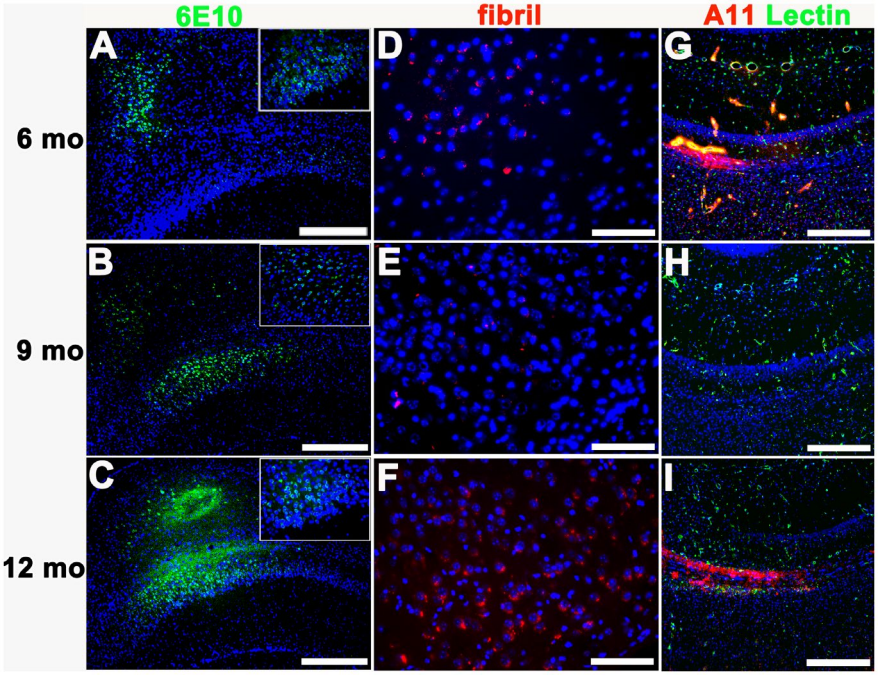

Figure 4. *Various expression pattern of Aβ using different antibodies in AD mice brain.* (**A-C**) The cerebral cortex and hippocampus sections from 3xTg-AD mice were stained by 6E10 (Green) at the ages of 6 mo (**A**), 9 mo (**B**), and 12 mo (**C**). The rectangle shows the magnified area of the hippocampus CA1 regions. (**D-F**) The hippocampus areas stained by anti-Aβ fibril antibodies (Red) at the ages of 6 mo (**D**), 9 mo (**E**), and 12 mo (**F**). (G-I) The high molecular weight Aβ oligomers in CA1 regions of hippocampus areas were stained with A11 antibody at the ages of 6 mo (**G**), 9 mo (**H**), and 12 mo (**I**). Green, Lectin labeled blood vessels; Blue, Hoechst 33342 stained nuclear. Scale bar, 50 μm in **A-C** and **G-I**, 10 μm in **D-F**.

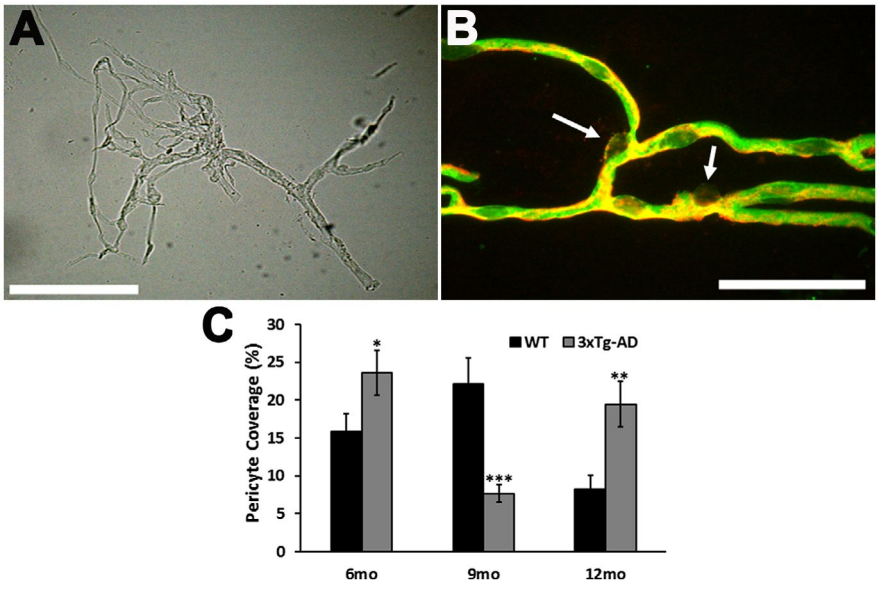

Figure 5. *Percentage of pericytes coverage in the WT and AD mice.* (**A**) The phase contrast image showed the morphology and purification of isolated microvessels. (**B**) The endothelial cells and pericytes of isolated capillaries were labeled with Lectin (green) and PDGFRβ (red) antibody, respectively, in AD mice. Scale bar, 10 μm in **A**, 5 μm in **B**. Arrows indicated pericytes. (**C**) Quantitative comparison of pericytes coverage of capillaries profiles between WT and AD (3xTg-AD) mice at the ages of 6 through 12 mo (n = 6 animals/group). Error bars = SEM; $*P < 0.05$, $**P < 0.01$, $***P < 0.001$, Student's *t* test.

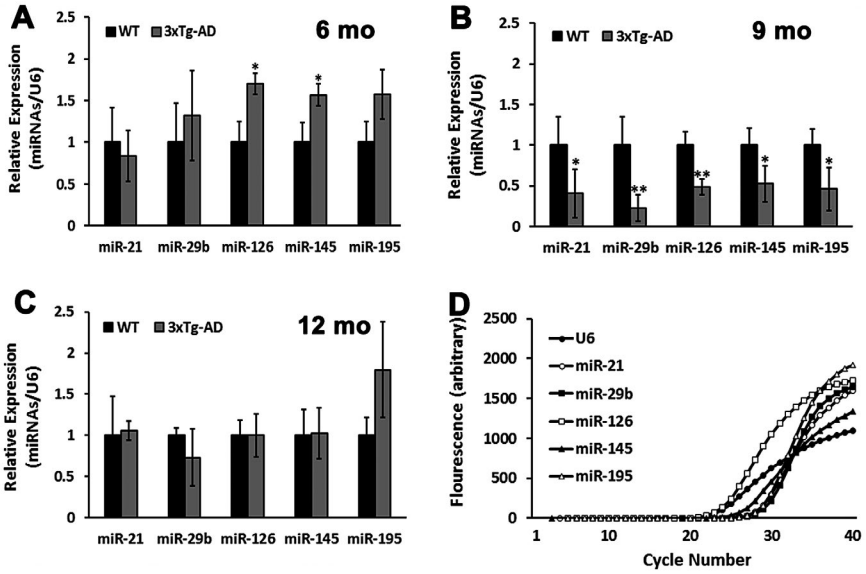

Figure 6. *Comparative expressions of 5 miRNAs in isolated capillaries.* (**A-C**) The quantitative comparison of qPCR results of 5 miRNAs levels in isolated capillaries of WT and AD (3xTg-AD) mice at 6 mo (**A**), 9 mo (B), 12 mo (**C**) (n = 6 animals/group). (**D**) The abundant of 5 miRNAs in isolated capillaries showed as a representative result of threshold cycle numbers from a WT animal of 9 mo. Error bars = SEM; $*P < 0.05$, $**P < 0.01$, Student's *t* test.

amongst the 5 selected miRNAs, which means greater abundance in isolated capillaries. This is consistent with the facts that miR-126 and miR-145 are mainly expressed in endothelial cells (ECs) and pericytes, respectively (33, 59). Notably, the levels of miR-126 and 145 were significantly and consistently changed among the selected vessel miRNAs in our study. Our functional studies on middle cerebral arteries (MCAs) from 3xTg-AD and WT mice aged 20 mo using pressure myography techniques indicate there are no obvious changes on vessel SMCs function that was assessed by MCA contractions to 60 mM KCl and 10 μM phenylephrine. EC-dependent relaxations to acetylcholine were reduced in MCA from 3xTg-AD mice. (Figure S2). Hence, we speculate that the function of ECs was mostly impacted by Aβ deposit in 3xTg mice. Combined with our inhibitor results (data not shown), we propose the levels of miRNAs, particularly miR-126, in isolated capillaries is strongly correlated with the clearance of Aβ from the perivascular space in 3xTg mice.

Ghrelin elevated miRNAs promoted Aβ oligomers clearance at 9mo in the AD mice brain

As compared with the vehicle administration, the percentage of pericyte coverage increased significantly ($P < 0.001$) in AD mice treated with ghrelin (Figures 7A-C). A significant increase in expression levels of 2 capillary miRNAs (miR126 and 145, $P < 0.05$) from the hippocampus and cerebral cortex were observed with ghrelin treatment as compared to saline-treated AD mice (Figure 7D). In contrast, compared to vehicle-treated AD brains, a significantly lower level of Aβ oligomers were seen in ghrelin-treated AD brains ($P < 0.05$) (Figures 7E-F). Meanwhile, the expressional levels of transporters that mediate Aβ to transport across the BBB, namely LRP1, RAGE and Mrd1, were detected by measuring the percentages of their relative expression in the isolated capillaries. Our data reveal that the relative expression of RAGE significantly declined ~10% in AD mice with ghrelin treatment compared to the saline-injected group (Figures 8D,G), meaning the influx of Aβ decreased after ghrelin administration may cause the lower levels of Aβ oligomers observed in the ghrelin group.

DISCUSSION

We observed increased cerebrovascular accumulation of Aβ oligomers accompanied by the increase in activated immune cells aligned in the cerebral vasculature, elevated pericyte coverage and up-regulation of vascular miRNAs (in particular, endothelium-specific miR-126 and 145) at 6 mo in 3xTg mice. These observations suggest that Aβ aggregation may stimulate the functional vasculature to drive Aβ oligomer elimination through the perivascular route in the early phase of AD mice. This leads to the transient decrease in Aβ oligomers and the restoration of the inflamed endothelium back to the quiescent phenotype in the next middle phase (9 mo), such as the diminishing of immune cell-positive vessels, the decline of pericyte coverage, and altered capillary miRNAs expression. When Aβ fibril starts to accumulate, the pericyte coverage and capillary miRNAs levels increase again to some extent, consistent with the fact that vascular activities can continuously contribute to the pathology of AD (58). Ghrelin-induced miRNAs expression triggered remarkably higher

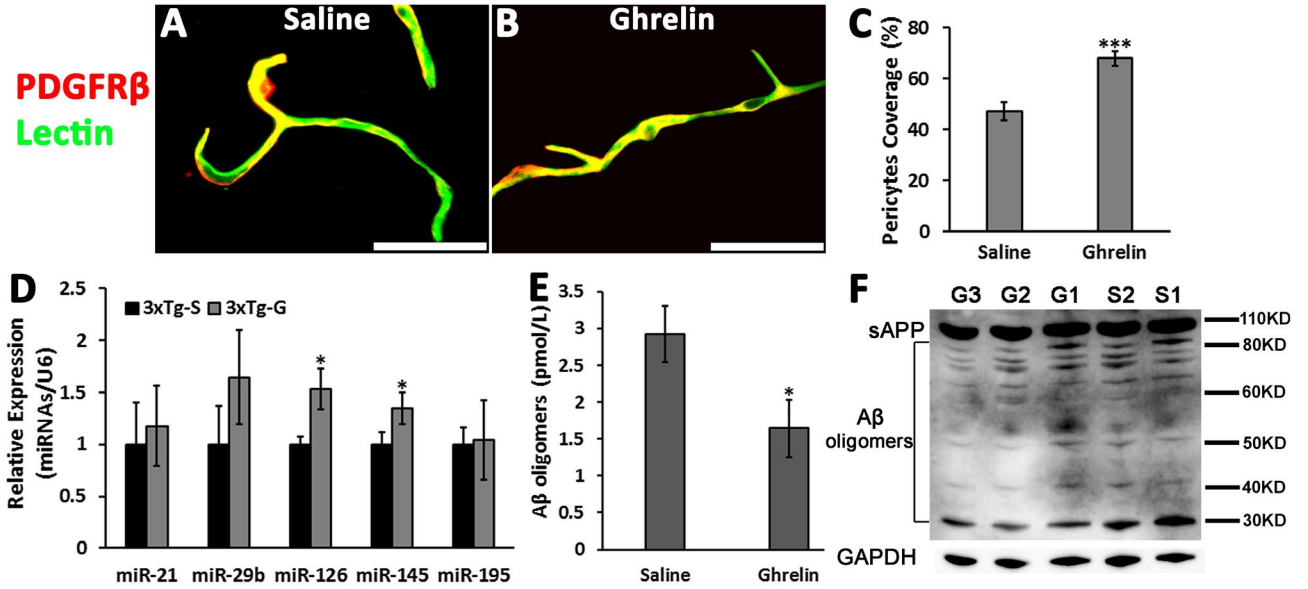

Figure 7. *Effect of Ghrelin on pericytes coverage, miRNAs and Aβ levels in 3xTg mice aged 9mo.* (**A**-**B**) Perictyes coverage of capillaries isolated from the hippocampus and cerebral cortex of 3xTg mice injected by vehicle (**A**, saline) or ghrelin (**B**). Green, Lectin labeled ECs; Red, PDGFRβ antibody stained perictyes. Scale bar, 5μm. (**C**) Quantified pericytes coverage in ghrelin and saline treated groups. (**D**) The expression of 5 selective microvessels miRNAs in ghrelin (3xTg-G) and saline (3xTg-S) injected AD mice. (**E**) Aβ oligomers were measured by ELISA. (**F**) Representative images for Aβ levels in the vessels-depleted hippocampus and cerebral cortex of 3xTg mice treated with ghrelin (G) or saline (S). sAPP, soluble APP; GAPDH, loading control. Error bars = SEM; $*P < 0.05$, $***P < 0.001$, Student's *t* test; n = 6-8 animals/group.

pericyte coverage and reduced Aβ oligomers during the period of lowering endothelium activities in the AD brain (9 mo), further supporting that the selected miRNAs are involved in regulating neurovascular activation and perivascular clearance of Aβ oligomers in AD pathogenesis. It is further implicated that the modulation of vascular miRNAs on activated vasculature and inflamed endothelium may play an important role in the pathogenesis of early AD.

ISF perivascular drainage exists as a route of metabolic byproduct removal from the brain parenchyma through perivascular spaces. Following the injection, tracers flow out of the parenchyma an hour later in the basement membranes of capillaries and in the extracellular matrix between the smooth muscle layer of the tunica media of arteries, but not along perivenous spaces (54). Damage to the brain microvasculature may affect Aβ perivascular elimination, promoting cerebrovascular Aβ aggregates, in turn inducing loss of vascular function and impairing angiogenesis. Aβ is present in small amounts of the normal brain (64) and in cerebral arteries of young human individuals (52). Failure of Aβ clearance appears to be a major factor in the pathogenesis of the more common late-onset sporadic AD (>95% AD cases) (63). Therapeutic strategies that facilitate the elimination of Aβ along the walls of blood vessels will expedite the discovery of novel drug targets.

Results gained from these 3xTg mice revealed the high-level of vascular adhesion molecules and various inflammatory factors were found in hippocampus and cortex at 6 mo of age (58, 68). In the early phase of the 3xTg-AD mouse model, deposits of Aβ may stimulate the inflamed BBB as a self-defense system to prevent further impairment in CNS. Combined with our findings on young and middle-aged animals, we speculate that the synthetic/activated phenotype of brain blood vessels is a form of "self-protection" against Aβ deposition in the brain, resulting in the partial clearance/degradation of Aβ by macrophages or immune cells. The protective role of extravagated macrophages, monocytes and T cells into the brain parenchyma has been demonstrated to facilitate the elimination of Aβ during the early phase of AD (58). The Aβ-initiated inflammation and function modification of cerebral vasculature exacerbate the disease process culminating in neuronal injury at late AD. Therefore, various investigators have proposed that blocking the migration of immune system cells into cerebral vasculature and the modification of BBB via inhibiting vascular activation may inhibit the progression of neurodegeneration and cognitive decline as a result of the neuronal toxicity of inflammatory factors, proteases and other noxious mediators released by activated brain endothelium (58, 68). Nonetheless, the boost of immune activities surrounding blood vessels and promotion of the vascular activation in early/middle AD will be beneficial for both inhibiting of Aβ deposition and postpone the occurrence of AD manifestations.

This 3xTg mouse model is a more complete model of AD that develop both Aβ and tau pathogenesis than most previous mouse strains. Our Aβ temporal profile confirmed the findings of the Laferla group (the first lab to develop 3xTg-AD mice strain) (6, 43) that Aβ deposit accumulated

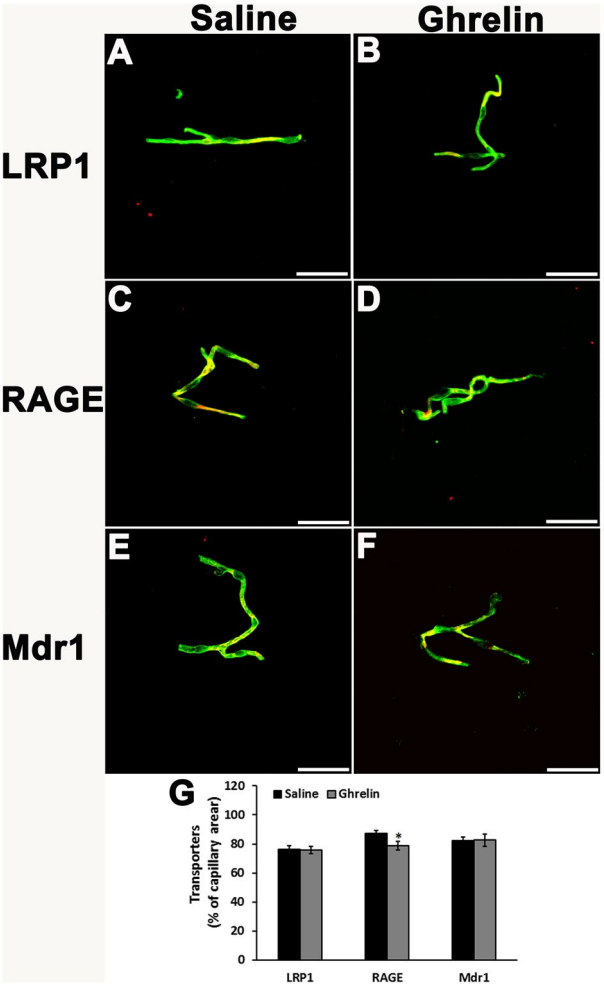

Figure 8. *Ghrelin treatment diminished the expression of RAGE.* (A-F) Representative of images of LRP1 (A and B), RAGE (C and D) and Mdr1 (E and F) staining in isolated capillaries from saline (A, C and E) or ghrelin (B, D and F) animals. (G) The percent area of lectin-positive microvessels occupied by LRP1, RAGE and Mdr1 immunofluorescent signals were quantified in saline and ghrelin treated 3xTg mice. Error bars = SEM; **P* < 0.05, Student's *t* test; n = 6-8 animals/group.

in an age-dependent manner and Aβ oligomer dramatically reduced at 9 mo. They proposed Aβ fibrillization may account for the reduction of oligomers (44). Our observations of robust Aβ fibril immunofluorescent signals in the hippocampus at 12 mo in 3xTg mice (Figure 4F) seem to support the increase in Aβ fibrillization. However, the levels of Aβ in the central nervous system (CNS) not only depend on production and fibrillization, but also on neurovascular clearance and degradation by diverse proteases in the brain parenchyma and blood. Higher immune activities from 3xTg mice aged 6 mo reported in previous studies (27, 68) and the transiently declined Aβ oligomers after 6 mo in these triple-transgenic mice, raised our curiosity and prompted us to verify the hypothesis that vascular activation and vessel miRNAs may be involved in the metabolism mechanism of Aβ oligomer clearance through the cerebral vasculature. Our findings suggest the dynamic deposits and drainage of Aβ is directly associated with early activation of cerebral vasculature and the endothelium functional regulation. The clearance of Aβ through the cerebral vasculature and BBB functional regulation at the early stage may be mediated by the intracellular gene regulation in the vascular wall, which could be modulated by capillary miRNAs in the younger 3xTg-AD mice brains.

Pericytes are cells uniquely located in neurovascular unit between ECs of BBB. These cells play a critical role in the modulation of the neurovascular homeostasis, including maintenance of brain microvascular stability, blood flow regulation, and clearance of toxic molecules (66, 72). The integrity of BBB is maintained by the interaction between ECs and pericytes. ECs secrete PDGF-β to recruit pericytes to survive and, in turn, pericytes regulate ECs by releasing signaling molecules to maintain tight junctions (45). The detachment of pericytes from ECs and loss from capillaries in both hippocampus and cortex causes neurovascular degeneration (41, 66). Our data showed pericyte coverage varied in line with the temporal profile of Aβ in 3xTg mice. Aβ deposit in the perivascular space at 6 mo might trigger up-regulation of vascular miRNAs, which activate the endothelium and recruit more pericytes to attach to ECs, accelerating the elimination of Aβ oligomers from the brain parenchyma and eventually lowering Aβ accumulation at 9 mo.

miRNAs can contribute to regulation of the BBB function and orchestrate the various endothelium responses at the post-transcriptional levels (36) in normal and disease brains (39, 49). This work, for the first time, demonstrated the epigenetic modulation of vascular miRNAs on cerebrovascular dysfunction in AD progression and contributes to the understanding of AD pathology. As a powerful agent to regulate multiple molecular cascades and complex multi-factorial diseases, miRNAs have emerged as a class of promising targets for therapeutic intervention (32, 61). Higher concentrations of oligonucleotide chemicals of miRNA modulators have been shown to affect ECs and capillaries surrounding cells in numerous cardiovascular studies (57). miRNA modulators in the blood can reach their targets, namely ECs and pericytes, much more easily than other potential therapies targeting neuronal or glial cells.

The modulation of 5 selected miRNAs on vascular remodeling and BBB integrity have been revealed previously. For example, miR-195 was significantly downregulated in rat brains after MCA occlusion and in hypoxia-induced human umbilical vein endothelial cells (69). miR-195 can inhibit human EPCs (endothelial progenitor cells) proliferation, migration, and angiogenesis under hypoxia via targeting vascular endothelial growth factor A (VEGFA) (40), while miR-145 promoted EPCs proliferation and migration in mice with cerebral infarction through the c-Jun N-terminal kinases signaling pathway (71). miR-21, as both anti-and pro-angiogenic regulator, has been shown to significantly increase after ischemic stroke, exerting opposite effects on angiogenesis in

normoxia and hypoxia (9). In contrast, miR-21 inhibited apoptosis and promoted angiogenesis by blocking the expression of its target phosphatase and tensin homolog, and activating protein kinase B signaling during brain injury (21). In ischemic stroke, overexpression of miR-29b rescued BBB disruption by downregulating aquaporin 4 (62). Meanwhile, miR-29b improved BBB integrity by increasing the levels of matrix metallopeptidase 9 via suppressing DNA (cytosine-5)-methyltransferase 3β (36). miR-126 is implicated in several important aspects of vascular biology, such as angiogenesis, capillary formation, and vascular inflammation (36, 59). It has been demonstrated that miR-126 is a negative regulator for mitogen-activated protein kinase and phosphoinositide 3-kinases pathways via repression of sprouty-related EVH1 domain containing 1 and phosphoinositol-3 kinase regulatory subunit 2 to maintain vascular integrity and promote angiogenesis (18).

Over the past 10 years, ghrelin, discovered as a gastric hormone, has shown wider physiological roles in ischemia, traumatic brain injury, spinal cord injury, amyotrophic lateral sclerosis, epilepsy, Parkinson's disease, and AD (17). Ghrelin has been shown to exert neuroprotective effects on the AD brain and ameliorate declined cognition (17). Previously, no significant diminishment in Aβ plaque burden was observed in 5XFAD mice with ghrelin treatment (42). In contrast, our data indicated ghrelin not only upregulated vessel miRNAs, but also attenuated Aβ oligomer load in 3xTg mice aged 9 mo. LRP1 and Mdr1 are implicated in the effective efflux of Aβ from the brain parenchyma back to the periphery across the BBB (7, 31, 35, 56). RAGE, involved in amyloidosis, mediated the luminal to abluminal influx of Aβ at the BBB (11, 12, 16, 50). Tuan et al demonstrated the BBB influx/efflux of Aβ was regulated in an age-dependent fashion in 3xTg mice (15). The equilibration of Aβ peptides across BBB was not disrupted until the late stages of AD (18 mo). In our animals aged 9 mo, ghrelin treatment disrupted the balance of influx/efflux of Aβ and attenuated the accumulation of these toxic Aβ oligomers in the parenchyma, which may be partially caused by reduced expression of RAGE. Whether RAGE expression was directly or indirectly affected by ghrelin through vessel-specific miRNAs, however, still requires further investigation.

Our study highlights the important role of the regulation of vascular miRNAs in Aβ drainage from the parenchyma and provides new knowledge to better understand AD etiology. The expression of vessel miRNAs orchestrates accurate tuning of gene expression that contributes to cerebrovascular function and BBB integrity, further influencing the extracellular Aβ clearance. Further work will be needed to deliver single or multiple vessel-special miRNA(s) into cerebral vasculature and address the potential influence on the structure and function of brain vessels and efficacy on the clearance of soluble Aβ oligomers in AD animal models. The development of novel pharmacologic intervention aimed at altering the levels of cerebrovascular miRNAs will impact AD with heterogenic or epigenetic origin. Direct transport of blood vessel-specific miRNA modulators can be potentially used to control Aβ levels in the brain to treat AD manifestations and can be considered as an important and promising therapeutic approach. Therefore, the success of manipulation of vascular miRNA in AD mouse brains will stimulate the drug target discovery and facilitate the development of an effective and safe pharmaceutical intervention for clinical studies of this devastating disease.

CONCLUSIONS

In summary, selected vessel-specific miRNAs, particularly miR-126 and 145, were highly correlated with the soluble Aβ oligomers clearance of brain vessels and involved in the regulation of Aβ concentration in the brains of 3xTg-AD mice. This implicates the underlying modulation mechanism of cerebrovascular miRNAs in perivascular drainage of Aβ oligomers and brain endothelial activation. This work contributes to the understanding of AD pathophysiology and may provide a new idea for developing novel preventive and/or therapeutic strategies in AD treatment.

ACKNOWLEDGMENTS

This work was supported by California medical innovations institute internal funding (10034-000-410). We would like to thank Dr. Howard J. Federoff (Dean of the School of Medicine, University of California, Irvine, USA) for critically reading the manuscript.

CONFLICT OF INTEREST

The authors declare no conflict of interest.

DATA AVAILABILITY STATEMENT

The data that support the findings of this study are available from the corresponding author upon reasonable request.

REFERENCES

1. Alamri BN, Shin K, Chappe V, Anini Y (2016) The role of ghrelin in the regulation of glucose homeostasis. *Horm Mol Biol Clin Investig* **26**:3–11.
2. Amar F, Sherman MA, Rush T, Larson M, Boyle G, Chang L *et al* (2017) The amyloid-β oligomer Aβ*56 induces specific alterations in neuronal signaling that lead to tau phosphorylation and aggregation. *Sci Signal.* **10**(478):eaal2021.
3. Bakker ENTP, Bacskai BJ, Arbel-Ornath M, Aldea R, Bedussi B, Morris AWJ *et al* (2016) Lymphatic clearance of the brain: perivascular, paravascular and significance for neurodegenerative diseases. *Cell Mol Neurobiol* **36**:181–194.
4. Bell RD, Winkler EA, Sagare AP, Singh I, LaRue B, Deane R, Zlokovic BV (2010) Pericytes control key neurovascular functions and neuronal phenotype in the adult brain and during brain aging. *Neuron* **68**:409–427.

5. Bell RD, Winkler EA, Singh I, Sagare AP, Deane R, Wu Z *et al* (2012) Apolipoprotein E controls cerebrovascular integrity via cyclophilin A. *Nature* **485**:512–516.
6. Billings LM, Oddo S, Green KN, McGaugh JL, LaFerla FM (2005) Intraneuronal Aβ causes the onset of early Alzheimer's disease-related cognitive deficits in transgenic mice. *Neuron* **45**:675–688.
7. Brenn A, Grube M, Peters M, Fischer A, Jedlitschky G, Kroemer HK, Warzok RW, Vogelgesang S. (2011) Beta-amyloid downregulates MDR1-P-glycoprotein (Abcb1) expression at the blood-brain barrier in mice. *Int J Alzheimers Dis* **2011**:1–6.
8. Cabral A, López Soto EJ, Epelbaum J, Perelló M (2017) Is ghrelin synthesized in the central nervous system? *Int J Mol Sci* **18**(9):638.
9. Chang C-H, Yen M-C, Liao S-H, Hsu Y-L, Lai C-S, Kuo Y-R, Hsu Y-L (2017) Dual role of MiR-21-mediated signaling in HUVECs and rat surgical flap under normoxia and hypoxia condition. *Int J Mol Sci* **18**(9):1917.
10. Chen Y, Liang Z, Blanchard J, Dai C-L, Sun S, Lee MH *et al* (2013) A non-transgenic mouse model (icv-STZ mouse) of Alzheimer's disease: similarities to and differences from the transgenic model (3xTg-AD mouse). *Mol Neurobiol* **47**:711–725.
11. Deane R, Wu Z, Zlokovic BV (2004) RAGE (yin) versus LRP (yang) balance regulates alzheimer amyloid beta-peptide clearance through transport across the blood-brain barrier. *Stroke* **35**:2628–263.
12. Deane R, Du Yan S, Submamaryan RK, LaRue B, Jovanovic S, Hogg E *et al* (2003) RAGE mediates amyloid-β peptide transport across the blood-brain barrier and accumulation in brain. *Nat Med* **9**:907–913.
13. Delay C, Hébert SS (2011) MicroRNAs and Alzheimer's disease mouse models: current insights and future research avenues. *Int J Alzheimer's Dis* **2011**:e894938.
14. Dissing-Olesen L, Hong S, Stevens B (2015) New brain lymphatic vessels drain old concepts. *EBioMedicine* **2**:776–777.
15. Do TM, Dodacki A, Alata W, Calon F, Nicolic S, Scherrmann J-M *et al* (2016) Age-dependent regulation of the blood-brain barrier influx/efflux equilibrium of amyloid-β peptide in a mouse model of Alzheimer's disease (3xTg-AD). *J Alzheimers Dis* **49**:287–300.
16. Donahue JE, Flaherty SL, Johanson CE, Duncan JA, Silverberg GD, Miller MC *et al* (2006) RAGE, LRP-1, and amyloid-beta protein in Alzheimer's disease. *Acta Neuropathol (Berl)* **112**:405–415.
17. Dos Santos VV, Rodrigues ALS, De Lima TC, de Barioglio SR, Raisman-Vozari R, Prediger RD (2013) Ghrelin as a neuroprotective and palliative agent in Alzheimer's and Parkinson's disease. *Curr Pharm Des* **19**:6773–6790.
18. Fish JE, Santoro MM, Morton SU, Yu S, Yeh R-F, Wythe JD *et al* (2008) miR-126 regulates angiogenic signaling and vascular integrity. *Dev Cell* **15**:272–284.
19. Frost S, Martins RN, Kanagasingam Y (2010) Ocular biomarkers for early detection of Alzheimer's disease. *J Alzheimers Dis* **22**:1–16.
20. Fu L, Shi Z, Luo G, Tu W, Wang X, Fang Z, Li X (2014) Multiple microRNAs regulate human FOXP2 gene expression by targeting sequences in its 3' untranslated region. *Mol Brain* **7**:71.
21. Ge X-T, Lei P, Wang H-C, Zhang A-L, Han Z-L, Chen X, Li S-H, Jiang R-C, Kang C-S, Zhang J-N. (2014) miR-21 improves the neurological outcome after traumatic brain injury in rats. *Sci Rep* **4**:6718.
22. Goodwill AG, Fu L, Noblet JN, Casalini ED, Sassoon D, Berwick ZC *et al* (2016) KV7 channels contribute to paracrine, but not metabolic or ischemic, regulation of coronary vascular reactivity in swine. *Am J Physiol Heart Circ Physiol* **310**:H693–704.
23. Grammas P, Martinez J, Sanchez A, Yin X, Riley J, Gay D *et al* (2014) A new paradigm for the treatment of Alzheimer's disease: targeting vascular activation. *J Alzheimers Dis* **40**:619–630.
24. Grinberg LT, Korczyn AD, Heinsen H (2012) Cerebral amyloid angiopathy impact on endothelium. *Exp Gerontol* **47**:838–842.
25. Hohsfield LA, Daschil N, Orädd G, Strömberg I, Humpel C (2014) Vascular pathology of 20-month-old hypercholesterolemia mice in comparison to triple-transgenic and APPSwDI Alzheimer's disease mouse models. *Mol Cell Neurosci* **63**:83–95.
26. Jackson AL, Levin AA (2012) Developing microRNA therapeutics: approaching the unique complexities. *Nucleic Acid Ther* **22**:213–225.
27. Janelsins MC, Mastrangelo MA, Oddo S, LaFerla FM, Federoff HJ, Bowers WJ (2005) Early correlation of microglial activation with enhanced tumor necrosis factor-alpha and monocyte chemoattractant protein-1 expression specifically within the entorhinal cortex of triple transgenic Alzheimer's disease mice. *J Neuroinflammation* **2**:23.
28. Joshi SR, Comer BS, McLendon JM, Gerthoffer WT (2012) MicroRNA regulation of smooth muscle phenotype. *Mol Cell Pharmacol* **4**:1–16.
29. Katare R, Rawal S, Munasinghe PE, Tsuchimochi H, Inagaki T, Fujii Y *et al* (2016) Ghrelin promotes functional angiogenesis in a mouse model of critical limb ischemia through activation of proangiogenic microRNAs. *Endocrinology* **157**:432–445.
30. Kress BT, Iliff JJ, Xia M, Wang M, Wei HS, Zeppenfeld D *et al* (2014) Impairment of paravascular clearance pathways in the aging brain. *Ann Neurol* **76**:845–861.
31. Kuhnke D, Jedlitschky G, Grube M, Krohn M, Jucker M, Mosyagin I *et al* (2007) MDR1-P-glycoprotein (ABCB1) mediates transport of Alzheimer's amyloid-β peptides—implications for the mechanisms of Aβ clearance at the blood-brain barrier. *Brain Pathol* **17**:347–353.
32. Lagos-Quintana M, Rauhut R, Yalcin A, Meyer J, Lendeckel W, Tuschl T (2002) Identification of tissue-specific microRNAs from mouse. *Curr Biol CB* **12**:735–739.
33. Larsson E, Fuchs PF, Heldin J, Barkefors I, Bondjers C, Genové G *et al* (2009) Discovery of microvascular miRNAs using public gene expression data: miR-145 is expressed in pericytes and is a regulator of Fli1. *Genome Med* **1**:108.
34. Lesné S, Koh MT, Kotilinek L, Kayed R, Glabe CG, Yang A *et al* (2006) A specific amyloid-beta protein assembly in the brain impairs memory. *Nature* **440**:352–357.
35. Liu Q, Zerbinatti CV, Zhang J, Hoe H-S, Wang B, Cole SL *et al* (2007) Amyloid precursor protein regulates brain apolipoprotein E and cholesterol metabolism through lipoprotein receptor LRP1. *Neuron* **56**:66–78.
36. Lopez-Ramirez MA, Reijerkerk A, de Vries HE, Romero IA (2016) Regulation of brain endothelial barrier function by microRNAs in health and neuroinflammation. *FASEB J* **30**:2662–72.
37. Louveau A, Da Mesquita S, Kipnis J (2016) Lymphatics in neurological disorders: a neuro-lympho-vascular component

of multiple sclerosis and Alzheimer's disease? *Neuron* **91**:957–973.
38. Maegdefessel L (2014) The emerging role of microRNAs in cardiovascular disease. *J Intern Med* **276**:633–644.
39. Millan MJ (2014) The epigenetic dimension of Alzheimer's disease: causal, consequence, or curiosity? *Dialogues Clin Neurosci* **16**:373–393.
40. Mo J, Zhang D, Yang R (2016) MicroRNA-195 regulates proliferation, migration, angiogenesis and autophagy of endothelial progenitor cells by targeting GABARAPL1. *Biosci Rep* **36**.
41. Montagne A, Barnes SR, Sweeney MD, Halliday MR, Sagare AP, Zhao Z *et al* (2015) Blood-brain barrier breakdown in the aging human hippocampus. *Neuron* **85**:296–302.
42. Moon M, Cha M-Y, Mook-Jung I (2014) Impaired hippocampal neurogenesis and its enhancement with ghrelin in 5XFAD mice. *J Alzheimers Dis JAD* **41**:233–241.
43. Oddo S, Caccamo A, Shepherd JD, Murphy MP, Golde TE, Kayed R *et al* (2003) Triple-transgenic model of Alzheimer's disease with plaques and tangles: intracellular Aβ and synaptic dysfunction. *Neuron* **39**:409–421.
44. Oddo S, Caccamo A, Tran L, Lambert MP, Glabe CG, Klein WL, LaFerla FM (2006) Temporal profile of amyloid-beta (Abeta) oligomerization in an in vivo model of Alzheimer disease. A link between Abeta and tau pathology. *J Biol Chem* **281**:1599–1604.
45. Park J-C, Baik SH, Han S-H, Cho HJ, Choi H, Kim HJ *et al* (2017) Annexin A1 restores Aβ1-42-induced blood–brain barrier disruption through the inhibition of RhoA-ROCK signaling pathway. *Aging Cell* **16**:149–161.
46. van Rooij E, Kauppinen S (2014) Development of microRNA therapeutics is coming of age. *EMBO Mol Med* **6**:851–64.
47. Rupaimoole R, Han H-D, Lopez-Berestein G, Sood AK (2011) MicroRNA therapeutics: principles, expectations, and challenges. *Chin J Cancer* **30**:368–370.
48. Sagare AP, Bell RD, Zhao Z, Ma Q, Winkler EA, Ramanathan A, Zlokovic BV (2013) Pericyte loss influences Alzheimer-like neurodegeneration in mice. *Nat Commun* **4**:2932.
49. Santulli G, Wronska A, Uryu K, Diacovo TG, Gao M, Marx SO *et al* (2014) A selective microRNA-based strategy inhibits restenosis while preserving endothelial function. *J Clin Invest* **124**:4102–4114.
50. Schmidt AM, Sahagan B, Nelson RB, Selmer J, Rothlein R, Bell JM (2009) The role of RAGE in amyloid-beta peptide-mediated pathology in Alzheimer's disease. *Curr Opin Investig Drugs Lond Engl 2000* **10**:672–680.
51. Shi Z, Luo G, Fu L, Fang Z, Wang X, Li X (2013) miR-9 and miR-140-5p target FoxP2 and are regulated as a function of the social context of singing behavior in zebra finches. *J Neurosci Off J Soc Neurosci* **33**:16510–16521.
52. Shinkai Y, Yoshimura M, Ito Y, Odaka A, Suzuki N, Yanagisawa K, Ihara Y (1995) Amyloid β-proteins 1–40 and 1–42(43) in the soluble fraction of extra- and intracranial blood vessels. *Ann Neurol* **38**:421–428.
53. Sweeney MD, Sagare AP, Zlokovic BV (2015) Cerebrospinal fluid biomarkers of neurovascular dysfunction in mild dementia and Alzheimer's disease. *J Cereb Blood Flow Metab* **35**:1055–1068.
54. Szentistványi I, Patlak CS, Ellis RA, Cserr HF (1984) Drainage of interstitial fluid from different regions of rat brain. *Am J Physiol* **246**:F835–F844.
55. Tarasoff-Conway JM, Carare RO, Osorio RS, Glodzik L, Butler T, Fieremans E *et al* (2015) Clearance systems in the brain-implications for Alzheimer disease. *Nat Rev Neurol* **11**:457–470.
56. Taylor DR, Hooper NM (2007) The low-density lipoprotein receptor-related protein 1 (LRP1) mediates the endocytosis of the cellular prion protein. *Biochem J* **402**:17–23.
57. Thum T (2012) MicroRNA therapeutics in cardiovascular medicine. *EMBO Mol Med* **4**:3–14.
58. Vinters HV, Pardridge WM (1986) The blood-brain barrier in Alzheimer's disease. *Can J Neurol Sci* **13**:446–448.
59. Wang S, Aurora AB, Johnson BA, Qi X, McAnally J, Hill JA *et al* (2008) The endothelial-specific microRNA miR-126 governs vascular integrity and angiogenesis. *Dev Cell* **15**:261–271.
60. Wang S-M, Fu L-J, Duan X-L, Crooks DR, Yu P, Qian Z-M *et al* (2010) Role of hepcidin in murine brain iron metabolism. *Cell Mol Life Sci CMLS* **67**:123–133.
61. Wang W-X, Huang Q, Hu Y, Stromberg AJ, Nelson PT (2011) Patterns of microRNA expression in normal and early Alzheimer's disease human temporal cortex: white matter versus gray matter. *Acta Neuropathol (Berl)* **121**:193–205.
62. Wang Y, Huang J, Ma Y, Tang G, Liu Y, Chen X *et al* (2015) MicroRNA-29b is a therapeutic target in cerebral ischemia associated with aquaporin 4. *J Cereb Blood Flow Metab* **35**:1977–1984.
63. Weller RO, Djuanda E, Yow H-Y, Carare RO (2008) Lymphatic drainage of the brain and the pathophysiology of neurological disease. *Acta Neuropathol (Berl)* **117**:1–14.
64. Weller RO, Massey A, Newman TA, Hutchings M, Kuo Y-M, Roher AE (1998) Cerebral amyloid angiopathy: Amyloid β accumulates in putative interstitial fluid drainage pathways in Alzheimer's disease. *Am J Pathol* **153**:725–733.
65. Winkler EA, Bell RD, Zlokovic BV (2011) Central nervous system pericytes in health and disease. *Nat Neurosci* **14**:1398–1405.
66. Winkler EA, Sagare AP, Zlokovic BV (2014) The pericyte: a forgotten cell type with important implications for Alzheimer's disease? *Brain Pathol* **24**:371–386.
67. You L-H, Yan C-Z, Zheng B-J, Ci Y-Z, Chang S-Y, Yu P *et al* (2017) Astrocyte hepcidin is a key factor in LPS-induced neuronal apoptosis. *Cell Death Dis* **8**:e2676.
68. Zenaro E, Pietronigro E, Della Bianca V, Piacentino G, Marongiu L, Budui S *et al* (2015) Neutrophils promote Alzheimer's disease-like pathology and cognitive decline via LFA-1 integrin. *Nat Med* **21**:880–886.
69. Zhao W-J, Zhang H-F, Su J-Y (2017) Downregulation of microRNA-195 promotes angiogenesis induced by cerebral infarction via targeting VEGFA. *Mol Med Rep* **16**:5434–5440.
70. Zhao Y-S, Zhang L-H, Yu P-P, Gou Y-J, Zhao J, You L-H *et al* (2017) Ceruloplasmin, a potential therapeutic agent for Alzheimer's disease. *Antioxid Redox Signal* **28**:1323–1337.
71. Zheng L, Cheng W, Wang X, Yang Z, Zhou X, Pan C (2017) Overexpression of MicroRNA-145 ameliorates astrocyte injury by targeting aquaporin 4 in cerebral ischemic stroke. *BioMed Res Int* **2017**:1–9.
72. Zlokovic BV (2011) Neurovascular pathways to neurodegeneration in Alzheimer's disease and other disorders. *Nat Rev Neurosci* **12**:723–738.

SUPPORTING INFORMATION

Additional supporting information may be found in the online version of this article at the publisher's web site:

Figure S1. Total 11 cerebral capillaries miRNAs were screened. (A) The quantitative comparison of qPCR results of 11 miRNAs levels in isolated microvessels of WT and AD mice (n = 3–5 animals/group). Only 3 miRNAs, i.e. miR-126, 145 and 195 were significantly upregulated in 3xTg mice aged 5 months old (5 mo) compared with WT mice at the same age. No expression for miR-199 and 208 was found in either WT or 3xTg mice brain capillaries. (B) The abundant of 11 miRNAs in isolated capillaries showed as a representative result of threshold cycle numbers from a WT animal of 6 mo. Error bars = SEM; $*P < 0.05$, $**P < 0.01$, Student's *t* test.

Figure S2. Cerebrovascular reactivity in aged (20 mo) 3xTg-AD mice. Middle cerebral arteries were studied using pressure myography techniques (60 mm Hg). (A). Contractions to 60 mM KCl were similar in WT and 3xTg-AD mice aged 20 mo, indicating that vessels smooth muscle cells function was intact. (B). Relaxation to acetylcholine (ACh) was impaired in aged 3xTg-AD mice, indicating endothelial dysfunction. Error bars = SEM, n = 2–3 animals/group.